Nonlinear Ultrafast Spin Scattering in the Skyrmion Phase of Cu_{2}OSeO_{3}

M. C. Langner, S. Roy, S. W. Huang, J. D. Koralek, Y.-D. Chuang, G. L. Dakovski, J. J. Turner, J. S. Robinson, R. N. Coffee, M. P. Minitti, S. Seki, Y. Tokura, and R. W. Schoenlein

Phys. Rev. Lett. **119**, 107204 — Published 7 September 2017
DOI: 10.1103/PhysRevLett.119.107204

Nonlinear Ultrafast Spin Scattering in the Skyrmion Phase of Cu_2OSeO_3

M.C. Langner,[1] S. Roy,[2] S-H. Huang,[2] J.D. Koralek,[3] Y.-D. Chuang,[2] G.L. Dakovski,[3] J.J. Turner,[3] J.S. Robinson,[3] R.N. Coffee,[3] M.P. Minitti,[3] S. Seki,[4,5] Y. Tokura,[4,6] and R. W. Schoenlein[1,3]

[1]*Materials Science Division, Lawrence Berkeley National Laboratory, Berkeley, CA 94720, USA*
[2]*Advanced Light Source, Lawrence Berkeley National Laboratory, Berkeley CA 94720, USA*
[3]*Linac Coherent Light Source, SLAC National Accelerator Laboratory, Menlo Park, California 94720, USA*
[4]*RIKEN, Center for Emergent Matter Science, Wako 351-0198, Japan.*
[5]*PRESTO, Japan Science and Technology Agency, Tokyo 102-0075, Japan.*
[6]*Department of Applied Physics, University of Tokyo, Tokyo 113-8656, Japan.*
(Dated: August 2, 2017)

Ultrafast X-ray scattering studies of the topological skyrmion phase in Cu_2OSeO_3 show the dynamics to be strongly dependent on the excitation energy and density. At high photon energies, where the electron-spin scattering cross section is relatively high, excitation of the topological skyrmion phase shows a non-linear dependence on the excitation density, in contrast to the excitation of the conical phase which linearly dependent on excitation density. The excitation of the skyrmion order parameter is nonlinear in the magnetic excitation resulting from scattering during electron-hole recombination, indicating different dominant scattering processes in the conical and skyrmion phases.

PACS numbers: 12.39.Dc, 78.70.Ck

Topologically protected states in a wide variety of condensed matter systems are of interest due to both new emergent physics and the potential in device applications [1–5]. One example of these topological states is the skyrmion, which is a particle-like excitation on a ferromagnetic background that forms as a twisted knot of spins in a regular hexagonal lattice [6]. The formation of the skyrmion lattice depends on a delicate balance between multiple interactions. For example, in chiral magnets such as MnSi, the skyrmion phase originates from competition between symmetric $\vec{S}_i \cdot \vec{S}_j$ exchange and antisymetric $\vec{S}_i \times \vec{S}_j$ Dzyaloshinskii-Moriya interactions [6], creating a Bloch-type skyrmion lattice. In thin films, skyrmions appear due to competition between the exchange and dipolar interaction[7, 8].

The skyrmion phase appears only in the presence of an applied magnetic field and is generally stable within a narrow temperature range near the Neel temperature [1, 6]. Understanding fluctuations and dynamics of the order parameter are fundamentally important to determine the robustness of the topological particles to impulsive perturbations and hence may provide insight into their potential use in magnetic logic and storage applications[9]. Theoretical work predicts that the connected tetrahedron network in Cu_2OSeO_3 gives rise to a Goldstone mode as well as other higher energy modes [10]. Microwave spectroscopy and optical pump-probe techniques have shown the presence of different collective modes such as circulating and breathing modes [11–13]. While these studies show that skyrmions exhibit interesting dynamic properties, more direct evidence of the effect of intense perturbative impulse on the skyrmion lattice can be obtained if we probe at the skyrmion q-vector using x-rays while pumping the system with an optical impulse.

Here, we present ultrafast optical pump/x-ray probe measurements of the skrymion and conical order parameters in Cu_2OSeO_3. Ultrafast optical excitation provides impulsive perturbation of the spins, and time-resolved resonant x-ray scattering follows the resulting changes in the order parameter. For both the conical and skyrmion phase we found dynamics with multiple time scales ranging from picoseconds to several nanoseconds. At low pump fluences, the perturbation of the conical phase is linear with excitation fluence. However, the perturbation of the skyrmion phase is distinctly non-linear in the low-fluence regime.

Ultrafast optical measurements have provided important insight into the fundamental interactions of magnetic materials, including the ultrafast loss of magnetic order in ferromagnets, and optically-driven magnetic switching in ferrimagnets and alloys on the ultrafast time scale [16]. Optical switching in skyrmions was theoretically proposed through a topological inverse Faraday effect [17], and ultrafast methods therefore provide the opportunity for measuring the fundamental switching speed of a skyrmion. Additionally, order fluctuations are known to play a crucial role in the formation of the skyrmion phase [1, 6], and the study of ultrafast processes that disorder spin magnetic states remains an active field of research. Ultrafast methods allow for the measurement of how topology affects spin-scattering processes, which, as we show here, alters the efficiency with which spins are scattered during the decay of optically pumped electrons.

Among Bloch-type skyrmion materials with antisymmetric Dzyaloshinskii-Moriya interactions, Cu_2OSeO_3 is unique as the only electrically insulating material known to exhibit this phase [1]. Cu_2OSeO_3 is cubic in structure, with both trigonal bipyramidal CuO_5 and square pyramidal CuO_5. The local magnetic ordering is primarily ferrimagnetic (T_c= 60 K), with a net magnetization resulting from oppositely-oriented Cu spins with different oxygen bonding geometries [1, 18, 19]. Related to the insulating nature, and of interest for applications, Cu_2OSeO_3 is multiferroic [1], with magnetic-field induced ferroelectricity that promises a unique approach to con-

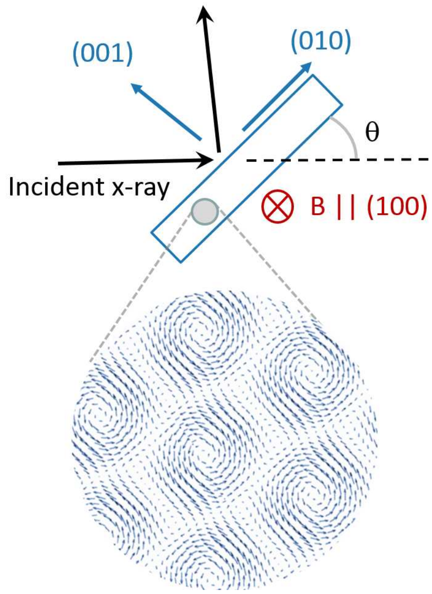

FIG. 1. Experimental scattering geometry. The magnetic field is applied perpendicular to the scattering plane. The skyrmion peaks appear as satellites to the (001) lattice peak.

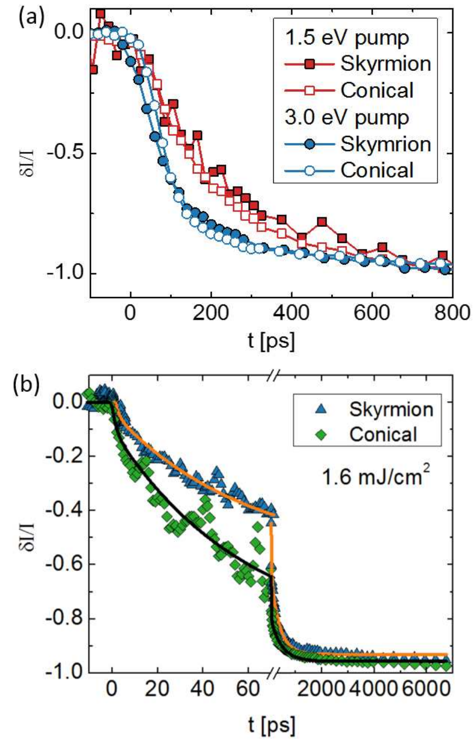

FIG. 2. (a) Comparison of dynamics for above gap (3.0 eV - circles) and below gap (1.5 eV - squares) excitation. Excitation density at both energies was 2.4 mJ/cm^2. 3.0 eV excitation results in faster dynamics in both conical (open symbols) and skyrmion (filled symbols) phases. The time-traces have been normalized to -1. (b) Ultrafast dynamics in skyrmion and conical phases with above-gap pump energy. Solid lines show three-timescale fits to the function represented in equation 1, with τ_i of 1.5 ps, 60 ps and 300 ps.

trol the skyrmion lattice.

Dynamics of the conical and skyrmion order parameters in Cu_2OSeO_3 were measured via time-resolved resonant x-ray scattering at the soft x-ray beamline at the Linac Coherent Light Source (LCLS) with 100 fs resolution and at BL6.02 at the Advanced Light Source (ALS) with 60 ps resolution [20, 21]. Both experiments probed the (1, 0, τ) and (1, τ, 0) scattering peaks, sensitive to conical and skyrmion order [11] with x-ray photon energy of 930 eV, resonant with the Cu L-edge. Dynamics were measured at 57.8 K, at the peak of the skyrmion scattering signal. A variable magnetic field was applied perpendicular to the scattering plane to access both the skyrmion and conical phases (Fig. 1) [22]. This geometry is chosen as a measure of the order parameter dynamics because it is insensitive to the linear and rotational in-plane motions of the hexagonal skyrmion lattice [23]. In both experiments, the sample was excited with 100 fs pump pulses at 1.5 and 3.0 eV, corresponding to excitation below and above the optical gap, which allows us to distinguish between magnetic excitation due to spin-lattice and electron-spin interactions.

Fig. 2(a) shows pump-probe data for the skyrmion and conical phases with 60 ps time resolution. In both phases, the primary effect of the excitation is a loss in x-ray scattering intensity corresponding to disruption of the ordered state. When excited below the optical gap at 1.5 eV, the loss of ordering occurs on a 300 ps time-scale for both magnetic phases, while with 3.0 eV excitation, the loss of ordering occurs on a significantly faster timescale, with dynamics faster than the probe resolution.

Fig. 2(b) shows dynamics of the skyrmion and conical scattering peak intensities with a pump energy of 3.0 eV on a 100 fs time-scale. The scattering intensity decays with timescales of 1.5 ps and 60 ps, in addition to the 300 ps timescale observed with 1.5 eV excitation.

Solid lines in Fig. 2(b) are exponential fits using these decay constants in the following model:

$$\delta I(t)/I = \sum_{i=1}^{3} \alpha_i e^{-t/\tau_i} \tag{1}$$

The time constants τ_i are the same for both conical and skyrmion phases.

The time scales of the magnetic excitations can be described within the three temperature model, in which magnetization dynamics occur due to energy transfer from photo-excited electrons to the spin system [24]. This is described by a set of equations:

$$C_i \frac{\delta T_i}{\delta t} = G_{i-j} \left(T_j - T_i\right). \tag{2}$$

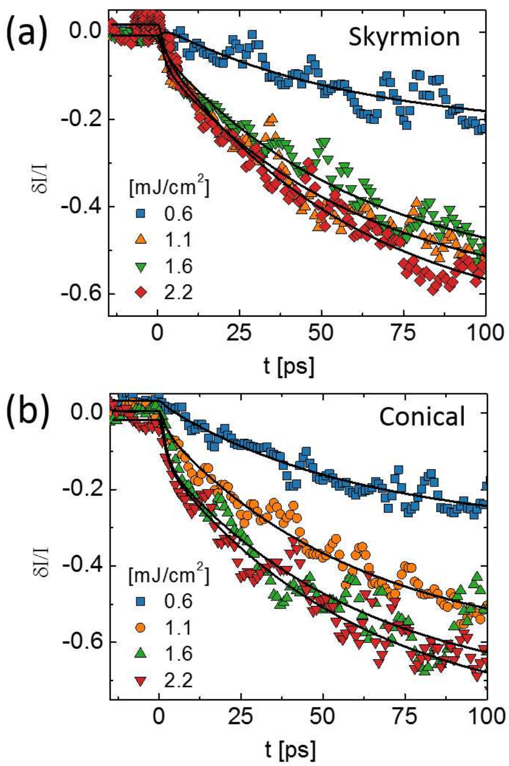

FIG. 3. Fluence dependence of the dynamics for the skyrmion (a) and conical (b) phases with 3 eV excitation.

The temperature of the spin, lattice, or electron system is given by T_i, C_i is the specific heat, and G_{i-j} is the coupling between systems. The subscripts indicate the relevant electron, spin, lattice baths (with subscripts e,s,l). The heating of the spin system from the excited electrons occurs either directly (G_{e-s}) or indirectly through phonon excitations (G_{l-s}). We consider three types of electron relaxations that transfer energy to the spin or lattice systems [22]. For 1.5 eV excitation, there is a decay from the mid-band virtual state back the ground state. For 3.0 eV excitation, there is an initial decay of electrons to the lowest unoccupied states of the conduction band and a subsequent decay of the electron-hole pairs across the band gap.

The photon energy dependence allows us to assign the observed time-scales to different scattering processes within this model. The 300 ps timescale observed in both 1.5 eV and 3.0 eV excitations is consistent with indirect excitation of the spin system through the lattice. For the 1.5 eV excitation, the dynamics are described entirely by this timescale, consistent with what has previously been observed in insulating magnets [16]. In contrast to metallic systems, the spin scattering cross section associated with relaxation from the excited virtual state to the ground state is small. The excess energy in the electrons is absorbed by the lattice (G_{e-l}), and the spin excitation occurs through subsequent spin-lattice interactions (G_{l-s}) [24, 25]. At higher fluences, we observe an almost complete loss of intensity on long time-scales, consistent with an increase of spin temperature above T_C.

At 3 eV, the pump photon energy is sufficient to excite electrons above the gap in the Cu d-level density of states [26], creating pseudo-stable electron-hole pairs. The decay of these pairs results in a faster loss of magnetic ordering, suggesting electron-spin scattering (G_{e-s}) during the electron decay from the conduction band. The similar time-scales in the magnetic phases indicate that the excited electron relaxation process is the same for the skyrmion and conical ordering. We conclude that for 3.0 eV excitation, the electron-spin coupling is relatively efficient, but the stability of the electron-hole pairs creates a bottleneck for the spin dynamics.

While the time-constants remain fixed as a function of fluence, the functional dependence of the differential loss of scattering intensity ($\delta I/I$) on short time-scales is the most striking distinction between the dynamics of the magnetic phases. Fig. 3 shows the fluence dependence of the skyrmion (a) and conical (b) dynamics with 3 eV excitation. The amplitudes of the differential scattering intensity (α_i in equation 1) is shown in Fig. 4 for the 1.5 ps (c) timescale. Figs. 4 (a) and (b) represent the loss of scattering intensity on 1 ns and 60 ps timescales, respectively. In both phases, the $\delta I/I$ associated with the faster 1.5 ps and 60 ps timescales saturates before complete loss of the magnetic order parameter. Complete loss of scattering intensity occurs only at high fluences on time-scales longer than 300 ps. In the conical phase, the short time-scale $\delta I/I$ initially increases proportionally with fluence, while in the skyrmion phase, $\delta I/I$ is super-linear before saturating at a higher remnant intensity than in the conical phase (4 (b)).

The lines in Fig. 4(b) are fits using saturation functions given by

$$\delta I_{con}(F) = \delta I_0 \left(1 - e^{-F/F_0}\right) \quad (3)$$

$$\delta I_{skx}(F) = \delta I_0^2 \left(1 - e^{-F/F_0}\right)^2 \quad (4)$$

for the conical and skyrmion phases, respectively. The fit parameters δI_0 and F_0 are the same for both phases, with a characteristic fluence (F_0) of 0.75 mJ/cm^2, corresponding to an excitation density of approximately one photon per ten unit cells.

The loss of scattering intensity is relatively small on the 1.5 ps time scale, and while the exact functional dependence cannot be discerned from the data, the associated $\delta I/I$ is non-linear in both phases (Fig. 4 (c)). We believe this timescale is caused by multiple photon absorption resulting in electron excitation significantly above the band gap, which is followed by electron-electron scattering processes that generate multiple carriers in the conduction band [16]. The fast time-scale implies relatively efficient spin scattering, while the reduction in ordering is relatively small due to the rarity of multi-photon absorption events.

Where the dynamics between skyrmion and conical phases differ significantly is the incomplete loss of magnetic ordering on a 60 ps timescale (Fig. 4 (b)). Similar saturation of

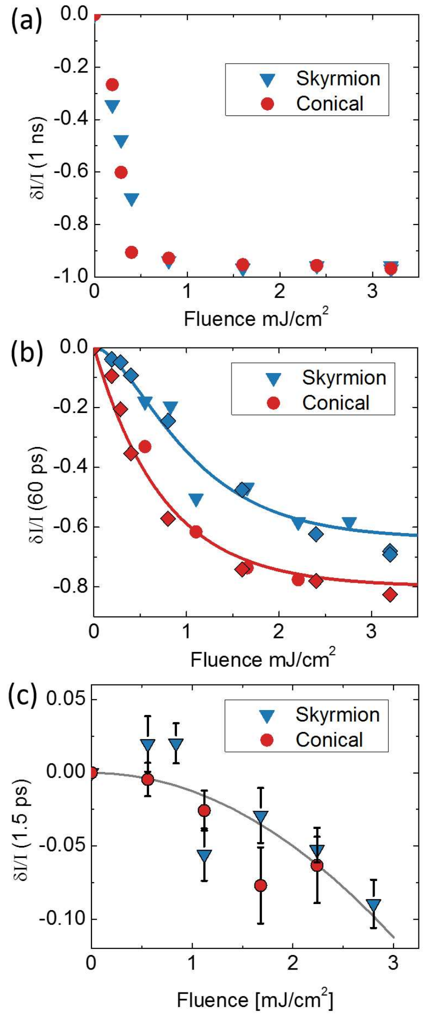

FIG. 4. Fluence dependence of the differential scattering signal with 3 eV excitation on a 1 ns (a) 60 ps (b) time-scales. Fit parameter α_i is shown for the 1.5 ps (c) time-scale component. Diamonds in (b) indicate the resolution-limited decay component measured with 60 ps resolution at the ALS. Other symbols are the total loss of intensity at 60 ps, corresponding to the sum of decay components α_i with 1.5 and 60 ps, measured with 100 fs resolution from the LCLS. Lines in (b) are fits to saturation functions as described in the text. The line in (c) represents an F^2 fluence dependence, which we postulate is the result of multiphoton absorption.

photo-induced magnetic disorder has been reported in ferromagnets on ultrafast time-scales and described as an effect of photo-induced filling of Stoner-like bands [27]. The saturation behavior occurs through the depletion of available optical transitions within an energy of $h\nu$ of the initial electron distribution, where $h\nu$ is the pump photon energy, conserving an imbalance of majority and minority spins even at high excitation density.

The common time-scales for the different magnetic phases imply common mechanisms for electron scattering, while different fluence-dependent saturation functions given by equation 3 indicate a different efficiency for spin scattering during this process. In the conical phase, the spin scattering resulting from the electron decay is linear at low fluences, with a saturation at high-fluences due to band-filling effects. The fluence-dependent loss of magnetic ordering in the skyrmion phase scales as the square of that in the conical phase. The saturated reduction of the skyrmion order parameter also scales as the square of that in the conical phase, indicating that the process responsible for the nonlinearity occurs after the saturation; the excitation of the skyrmion order parameter is nonlinear in the magnetic excitation resulting from the electron decay.

There are multiple possible explanations for the nonlinearity. The conical/skyrmion to paramagnetic transitions are first-order [28, 29]. Reduction in scattering intensity could be explained by either spatially uniform reduction of the magnetic ordering through spin wave excitations or through the creation of disordered domains. A nonlinearity in the first-order skyrmion to disordered phase transition could indicate a higher latent heat for this transition than in the conical phase. However, we observe no change in the shape of the diffraction peak that would indicate the formation of large disordered domains. Additionally, no significant difference is reported between the conical and skyrmion latent heat, and in MnSi, the conical latent heat appears to be larger [28].

Alternatively, the nonlinearity could relate to the density of magnetic excitations that reduce the finite-q order parameters. The initial excitation of the spin system occurs through spin-flip processes, which then decay into lower-energy excitations of the order parameter. The magnetic dispersion relations are anisotropic [30, 31], and the observed dynamics in the x-ray scattering differ significantly from those in optical magnetic measurements of skyrmion materials [12, 13], which measure dynamics of the q=0 magnetization. This indicates low-energy excitations that are not evident in measurements at the skyrmion/conical wave vectors. Additionally, the measured skyrmion wave-vector is a projection of a planar structure, which relative to the one-dimensional ordering in the conical phase, has a higher dimensionality for the density of relevant magnetic excitations. At the skyrmion/conical wave vector, the relevant excitations are relatively high energy, and the higher dimensionality of the skyrmion phase corresponds to higher density of excitations at the measured wave vector, leading to the scaling observed between the skyrmion and conical dynamics.

In conclusion, we have demonstrated that ultrafast magnetic scattering differs between magnetic phases of different topology in Cu_2OSeO_3. The skyrmion phase is more robust to optical excitation even with excitation energies substantially larger than the free energy difference between phases. The primary excitations are de-localized spin wave excitations, which are generated on a time scale masked by the electron-hole recombination time. Additional studies on metallic materials, where excitations couple to spins on faster time scales may further elucidate the dynamical behavior of the skyrmion lattice in response to optical switching or photo-injected defects.

The work at LBNL, including experiments at ALS, was supported by the Director, Office of Science, Office of Basic Energy Sciences, of the U.S. Department of Energy under Contract No. DEAC02-05CH11231.

Use of the Linac Coherent Light Source (LCLS), SLAC National Accelerator Laboratory, is supported by the U.S. Department of Energy, Office of Science, Office of Basic Energy Sciences under Contract No. DE-AC02-76SF00515.

[1] S. Seki *et al.*, Science **336**, 198 (2012).
[2] A. O. Leonov, I. E. Dragunov, U. K. Rößler, and A. N. Bogdanov, Phys. Rev. E **90**, 042502 (2014).
[3] P. J. Ackerman, R. P. Trivedi, B. Senyuk, J. van de Lagemaat, and I. I. Smalyukh, Phys. Rev. E **90**, 012505 (2014).
[4] Y. Nahas, S. Prokhorenko, L. Louis, Z. Gui, I. Kornev, and L. Bellaiche, Nature Communications **6**, 8542 (2015).
[5] A. Yadav, C. Nelson, S. Hsu, Z. Hong, J. Clarkson, C. Schlepetz, A. Damodaran, P. Shafer, E. Arenholz, L. R. Dedon, D. Chen, A. Vishwanath, A. Minor, L. Chen, J. Scott, L. Martin, and R. Ramesh, Nature **520**, 198 (2016).
[6] S. Mülhbauer *et al.*, Science **323**, 915 (2009).
[7] M. Ezawa, Phys. Rev. Lett. **105**, 197202 (2010).
[8] X. Yu, M. Mostovoy, Y. Tokunaga, W. Zhang, K. Kimoto, Y. Matsui, Y. Kaneko, N. Nagaosa, and Y. Tokura, Proceedings of the National Academy of Sciences of the United States of America **109**, 8856 (2012).
[9] A. Fert, V. Cros, and J. a. Sampaio, Nature Nanotechnology **8**, 152 (2013).
[10] J. Romhányi, J. van den Brink, and I. Rousochatzakis, Phys. Rev. B **90**, 140404 (2014).
[11] Y. Onose, Y. Okamura, S. Seki, S. Ishiwata, and Y. Tokura, Phys. Rev. Lett. **109**, 037603 (2012).
[12] N. Ogawa, S. Seki, and Y. Tokura, Scientific Reports **5**, 9552 (2015).
[13] J. D. Koralek, D. Meier, J. P. Hinton, A. Bauer, S. A. Parameswaran, A. Vishwanath, R. Ramesh, R. W. Schoenlein, C. Pfleiderer, and J. Orenstein, Phys. Rev. Lett. **109**, 247204 (2012).
[14] J. Sampaio, V. Cros, S. Rohart, A. Thiaville, and A. Fert, Nature Nanotechnology **8**, 839 (2013).
[15] F. Jonietz *et al.*, Science **330**, 1648 (2010).
[16] A. Kirilyuk, A. V. Kimel, and T. Rasing, Rev. Mod. Phys. **82**, 2731 (2010).
[17] K. Taguchi, J.I. Ohe, and G. Tatara, Phys. Rev. Lett. **109**, 127204 (2012).
[18] J.-W. G. Bos, C. V. Colin, and T. T. M. Palstra, Phys. Rev. B **78**, 094416 (2008).
[19] M. Belesi, I. Rousochatzakis, H. C. Wu, H. Berger, I. V. Shvets, F. Mila, and J. P. Ansermet, Phys. Rev. B **82**, 094422 (2010).
[20] R. Alonso-Mori, C. Caronna, M. Chollet, R. Curtis, D. S. Damiani, J. Defever, Y. Feng, D. L. Flath, J. M. Glownia, S. Lee, H. T. Lemke, S. Nelson, E. Bong, M. Sikorski, S. Song, V. Srinivasan, D. Stefanescu, D. Zhu, and A. Robert, J. Synchrotron Rad. **22**, 152021 (2015).
[21] C. Bostedt, S. Boutet, D. M. Fritz, Z. Huang, H. J. Lee, H. T. Lemke, A. Robert, W. F. Schlotter, J. J. Turner, and G. J. Williams, J. Synchrotron Rad. **88**, 015007 (2016).
[22] See supplemental material.
[23] M. C. Langner, S. Roy, S. K. Mishra, J. C. T. Lee, X. W. Shi, M. A. Hossain, Y.-D. Chuang, S. Seki, Y. Tokura, S. D. Kevan, and R. W. Schoenlein, Phys. Rev. Lett. **112**, 167202 (2014).
[24] T. Ogasawara, K. Ohgushi, Y. Tomioka, K. S. Takahashi, H. Okamoto, M. Kawasaki, and Y. Tokura, Phys. Rev. Lett. **94**, 087202 (2005).
[25] B. B. Koopmans, G. Malinowski, F. Dalla Longa, D. Steiauf, M. Fähnle, T. Roth, M. Cinchetti, and M. Aeschlimann, Nature Materials **9**, 259 (2010).
[26] J. H. Yang, Z. L. Li, X. Z. Lu, M.-H. Whangbo, S.-H. Wei, X. G. Gong, and H. J. Xiang, Phys. Rev. Lett. **109**, 107203 (2012).
[27] D. Cheskis, A. Porat, L. Szapiro, O. Potashnik, and S. Bar-Ad, Phys. Rev. B **72**, 014437 (2005).
[28] A. Bauer, M. Garst, and C. Pfleiderer, Phys. Rev. Lett. **110**, 177207 (2013).
[29] V. A. Sidorov, A. E. Petrova, P. S. Berdonosov, V. A. Dolgikh, and S. M. Stishov, Phys. Rev. B **89**, 100403 (2014).
[30] J. Zang, M. Mostovoy, J. H. Han, and N. Nagaosa, Phys. Rev. Lett. **107**, 136804 (2011).
[31] O. Petrova and O. Tchernyshyov, Phys. Rev. B **84**, 214433 (2011).